JOURNAL OF CATALYSIS 21, 294–302 (1971)

Catalyst Characterization Studies on the Zn–Cr–Fe Oxide System

F. E. MASSOTH AND D. A. SCARPIELLO

Gulf Research & Development Company, Pittsburgh, Pennsylvania 15230

Received July 17, 1970

Basic catalyst characterization studies of the title system were carried out to gain insight into the unique nature of zinc–chromium ferrite for the oxidative dehydrogenation of butene to butadiene. Relative reactivities of the various oxides in hydrogen and butene at temperatures up to 550°C were determined by measuring catalyst weight loss in a flow, microbalance reactor.

The ease of reducibility of oxide in hydrogen decreases in the following order:

$$Fe_2O_3 > ZnFe_2O_4 > ZnCrFeO_4 = FeCrO_3 > ZnCr_2O_4 > ZnO > Cr_2O_3.$$

In butene, Fe_2O_3 and $FeCrO_3$ are reduced to lower-valence oxides, while $ZnFe_2O_4$, and $ZnCrFeO_4$ lose approximately 2 monolayers of oxygen. Noteworthy is the fact that the latter are selective catalysts for butene dehydrogenation.

In the presence of both butene and air at 350°C, the $ZnCrFeO_4$ catalyst at first rapidly gains weight, and then lines out. A carbonaceous deposit is present during the steady-state catalytic reaction while the catalyst remains essentially in the oxidized state. Regeneration in air returns the catalyst to its original weight.

A surface reaction sequence for the oxidation dehydrogenation involving an iron–oxygen radical active center is proposed.

INTRODUCTION

Many oxide catalysts have been evaluated for oxidative dehydrogenation of olefins (*1*). Recent studies have reported on conversion of butene to butadiene using bismuth molybdates (*2*), zinc–chromium–iron oxides (*3*), and many others (*4*). Various mixed-metal oxides have been studied at this Laboratory for the oxidative conversion of butene to butadiene. Of these, the ferrites, and especially zinc–chromium ferrite, have demonstrated high conversion and selectivity to butadiene (*5*).

The present study was initiated with the objective of improving our basic understanding of the catalyst function involved in this important oxidation process. The approach taken was to determine the reactivities of both the individual oxides and their various combinations in a reducing atmosphere of either hydrogen or butene. The basic technique used was that of the flow microbalance which affords a direct and continuous measurement of catalyst weight loss during the course of the reduction process. Other measurements were used to supplement these findings.

EXPERIMENTAL

The single oxides of Zn, Cr, and Fe were prepared by calcination of their corresponding nitrates at 540°C. Preparation of the binary and ternary oxides has been previously described (*5*). Catalysts were pretreated in nitrogen at reaction temperature for an overnight period to establish the same thermal history. A similar treatment in air did not appear to cause any significant difference in reactivity towards hydrogen or butene.

Butene-1, 99% purity, was used without further purification. Nitrogen was purified by passing over hot copper turnings to remove oxygen, followed by type 4A molecular sieves for dying. Ultrahigh-purity hydrogen was passed through a deoxo unit before drying with molecular sieves. Various partial pressures of mixtures were achieved by flow metering individual streams.

A continuous record of weight change was obtained by use of a Cahn microbalance in a flow system at atmospheric pressure. Sample weights varied from 100 mg to 2.5 g and were contained in a quartz bucket suspended from the balance arm. The assembly was enclosed in a quartz-tube reactor which was heated by a conventional furnace. Temperature control was within ±2°C of the desired temperature. Gas rates employed were 400 cm^3/min total flow. Quartz chips were located at the bottom of the reactor tube (inlet) to preheat the incoming gas stream. Small buoyancy corrections were applied to the weight changes by reference to a standard nitrogen flow before and after reaction.

Additional techniques employed to supplement the microbalance studies included: X-ray diffraction; BET surface area using krypton as adsorbate, and electron spin resonance (ESR).

Results

Reactivity in Hydrogen

To determine the relative reducibilities of the various oxides in hydrogen, thermogravimetric analyses (TGA) were run, where the temperature was increased at a constant heating rate of 3°C/min, and the corresponding weight loss recorded. Figure 1 depicts the ease of removal of oxygen from the various oxides. Ferric oxide is most readily reduced, with the initial reduction occurring at about 300°C. Reduction to metallic iron is complete at 425°C. $ZnFe_2O_4$ starts to react at 350°C and, as shown in the TGA plot, a plateau is reached in the vicinity of 450°C. At this stage, the iron is completely reduced to the metallic state. Above 500°C, the sample begins to lose weight again due to reduction of the ZnO and subsequent vaporization of metallic zinc, which deposits as a metallic mirror on the cool surface of the quartz reactor. ZnO itself is not readily reduced since reaction occurs at 525°C; at the maximum temperature of 540°C, zinc is vaporized. Reduction of $ZnCr_2O_4$ was initiated at 425°C, with Zn vaporization occurring at 540°C. Ferric ion in $FeCrO_3$ was slowly reduced so that at 540°C, an intermediate stage of reduction was reached where the empirical composition was $FeCrO_{2.5}$. It is probable that the resultant oxide was mainly a mixture of FeO and Cr_2O_3 at this point (*6*), although reduction was continuing. No appreciable reduction of chromic oxide occurred at temperatures up to 700°C. The temperatures for initiation of reduction for the simple oxides are close to those reported by Garner (*7*).

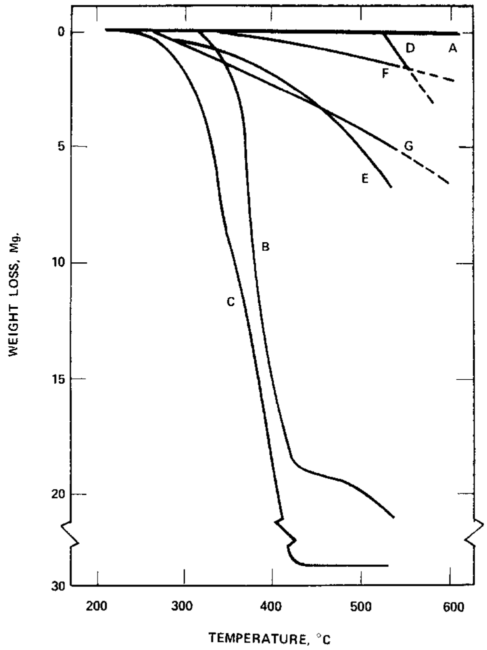

FIG. 1. TGA of ZnCrFe oxides ni H_2 with a 100 mg charge. Symbols: A, Cr_2O_3; B, $ZnFe_2O_4$; C, Fe_2O_3; D, ZnO; E, $FeCrO_3$; F, $ZnCr_2O_4$; G, $ZnCrFeO_4$.

In the case of the ternary oxide, $ZnCrFeO_4$, an initial loss in weight occurred at low temperature with evolution of water, a weight plateau being observed between 150 and 250°C. The loss was equivalent to about 2 monolayers of oxygen. Appreciable bulk reduction started at about 300°C and continued to 540°C. At the latter temperature, the assumed stoichiometry corresponded roughly to $2FeO \cdot 2ZnO \cdot Cr_2O_3$.

Above 540°C, the oxide continued to lose weight due to zinc reduction and volatilization, and possibly further reduction of iron.

An isothermal reduction of zinc–chromium ferrite catalyst was carried out at 400°C. Based on oxygen weight loss, the Fe^{3+} cation was reduced to Fe^{2+}. At this temperature, the oxides of zinc and chromium are not reducible by hydrogen. The catalyst was next regenerated in air at 350°C, and it returned to the fully oxidized state. The same reduction–oxidation cycle was repeated, and in both cases, the extent of reduction and oxidation was the same. Apparently, the iron in the spinel matrix is stable to reduction beyond the +2 state at moderate temperature. Initial rates of reduction in hydrogen showed that the second reduction proceeded at a faster rate than the first, indicating a change in the reactivity of the catalyst with prior reduction. An explanation for this is offered later.

Reactivity in Butene

In butene, the oxides that reduced all included iron. The others either did not react, or resulted in carbonaceous deposits. In general, carbonaceous deposition occurred at temperature above 500°C. Table 1 summarizes the results. Both Fe_2O_3 and $FeCrO_3$ reduced to lower valence-state iron. In the case of $ZnFe_2O_4$ and $ZnCrFeO_4$, only small weight losses were obtained signifying surface rather than bulk reduction. Only carbon formation was observed for the $ZnCr_2O_4$.

TABLE 1

BUTENE REDUCTIONS OF OXIDES

Oxide	Product	Temp. (°C)
Fe_2O_3	Fe_3O_4	400–540
$FeCrO_3$	Fe_3O_4, Cr_2O_3	540
$ZnCr_2O_4$	No reaction	400
	Carbon deposit	500
$ZnFe_2O_4$	Surface O loss	400
$ZnCrFeO_4$	Surface O loss	400
	Carbon deposit	500

The study of zinc–chromium ferrite reduction by butene was extended to larger sample size to magnify the surface reaction. A 2.5 g-sample of fresh catalyst was subjected to a sequence of gases, and Fig. 2 shows the corresponding weight changes. Initially, the charge was heated in N_2 to 120°C. Butene was introduced and a small increase in weight occurred. Butene was replaced by air and the temperature was increased to 350°C. The catalyst lost weight

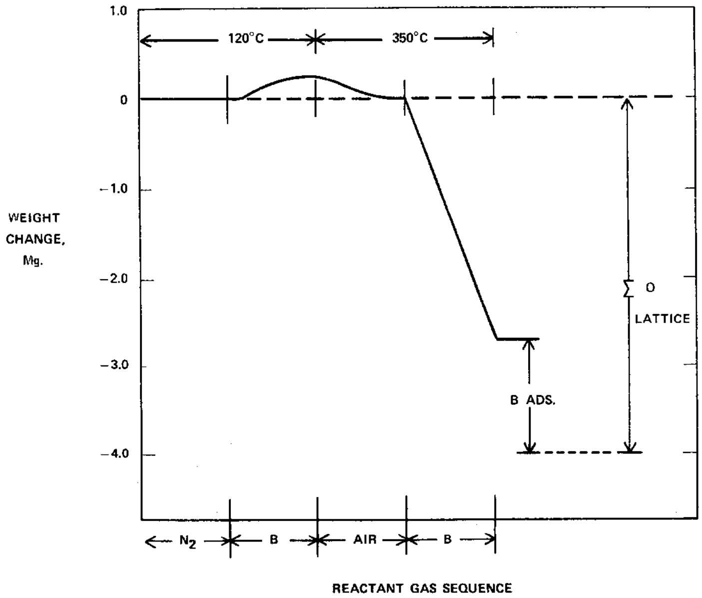

FIG. 2. Butene reduction of $ZnCrFeO_4$, 2.5 g charge, 2.0 m^2/g. Symbol B, 0.17 atm butene in N_2.

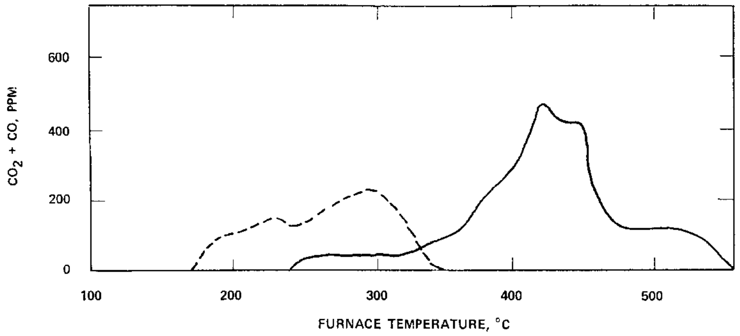

FIG. 3. Air regeneration of $ZnCrFeO_4$ vs. coked catalyst: ———, coked SiO_2–Al_2O_3 catalyst; and - - -, butene adsorbed on $ZnCrFeO_4$.

due to desorption and/or oxidation of the adsorbed butene. The initial oxidized state of the catalyst was attained at this point. A significant amount of oxygen was removed on next introducing butene into the reactor at the higher temperature. However, the weight loss observed must be corrected for olefin adsorption.* The adsorption correction was determined by increasing the temperature in air and measuring the formation of carbon oxides in the effluent gas by gas chromatography. The results are shown in Fig. 3 where the concentration of CO_2 plus CO is compared to that observed in the regeneration of a coked silica-alumina catalyst (*8*). Previous investigation has shown that two types of deposit are present on the latter catalyst: (1) an active surface species that oxidizes at low temperature 300–400°C; and (2) a bulk coke deposit that reacts in the 400–600°C range (*9*). For the ferrite catalyst, only a lower temperature regime (200–300°C) is involved in the oxidation of the carbon species, suggesting an adsorbed species rather than a true coke deposit to be present. ESR analysis of a similar sample before regeneration failed to detect any signal due to free carbon, confirming lack of a true coke structure (*10*). The measured carbon oxides, calculated as adsorbed butene** (1.4 mg), corresponds closely to a monolayer coverage on the catalyst using 38 Å^2 for the area of an adsorbed butene molecule (*11*). Correcting for the adsorbed olefin, the total amount of oxygen lost from the sample was 4.1 mg, which corresponds to the removal of about two layers of oxygen from the catalyst surface, assuming close-packed oxide ions (6.8Å^2).

The two oxide layers lost are attributed to one layer each of lattice oxide with attendant reduction of surface iron from Fe^{3+} to Fe^{2+} and of strongly chemisorbed oxygen (active). Evidence that the reduced state of the catalyst in butene is associated with a lower valence of Fe was derived from ESR measurements. A broadening of one-half of the Cr^{3+} signal was observed, indicating the presence of ferromagnetic material. This is of course in accord with our supposition that Fe^{3+} at the surface is being reduced to Fe^{2+} in butene, the ferromagnetism arising from the Fe^{3+} bulk–Fe^{2+} (surface) couple.

A separate experiment was undertaken to prove the existence of chemisorbed oxygen on the fresh zinc–chromium ferrite catalyst. The catalyst was heated in an air-free nitrogen stream to 800°C and subsequently cooled to 500°C, still maintaining the nitrogen atmosphere. Upon introduction of air, a weight gain ensued corresponding closely to a monolayer adsorption of oxygen. We ascribe the oxygen pickup to formation of a surface chemisorbed oxygen species. That the active oxygen was strongly held was evidenced by its only being partly removed upon subsequent replacement of the air with nitrogen at 500°C, considerably higher temperatures being required to remove it.

---

* We include in this term: butene, butadiene, and any low molecular weight olefinic-type products.

** Approximately the same value is obtained assuming butadiene as the adsorbed species.

Reintroduction of air at 500°C restored the catalyst to its former oxidized state.

Reactivity in Butene and Air

Since a continuous process using air involves replenishment of catalyst oxygen lost by butene reaction, a butene-air cycle was studied in the microbalance. As a supplementary experiment, a temperature profile was obtained under the same conditions in another reactor of identical geometry, but containing a microthermocouple inserted into the catalyst sample. Figure 4 illustrates the reaction sequence with the upper plot depicting weight changes, and the lower, the corresponding temperature changes. The initial step consisted of a nitrogen pretreatment to 350°C. On introduction of butene at a partial pressure of 0.17 atm, the catalyst lost weight due to removal of surface oxygen. Counteracting this weight loss was a weight gain due to olefin adsorption, the net effect being a decrease in catalyst weight. Also, a small exothermic heat effect was noted. The temperature rise fell rapidly to zero signifying termination of the surface reaction. The next step was the addition of air at a butene-to-oxygen ration of 1.5. A relatively large increase in weight ensued and a significant rise in temperature accompanied this step. There was a slight leveling off from the maximum temperature reached, but a positive temperature difference persisted due to the exothermic catalytic reaction. With the removal of air, a rapid decline in temperature took place, indicating that the catalytic reaction was essentially terminated. Concurrently, the sample lost weight. The residual weight above the base level is due to the accumulation of a carbonaceous deposit on the catalyst surface. Removal of butene from the stream, leaving nitrogen, caused no further weight loss, showing the deposit to be irreversibly adsorbed. The final step involved admission of air; this resulted in a slight but rapid increase in weight due to rapid oxygen adsorption, followed by a decrease in weight from burn-off of the carbonaceous deposit, with return to the original weight. This step was accompanied

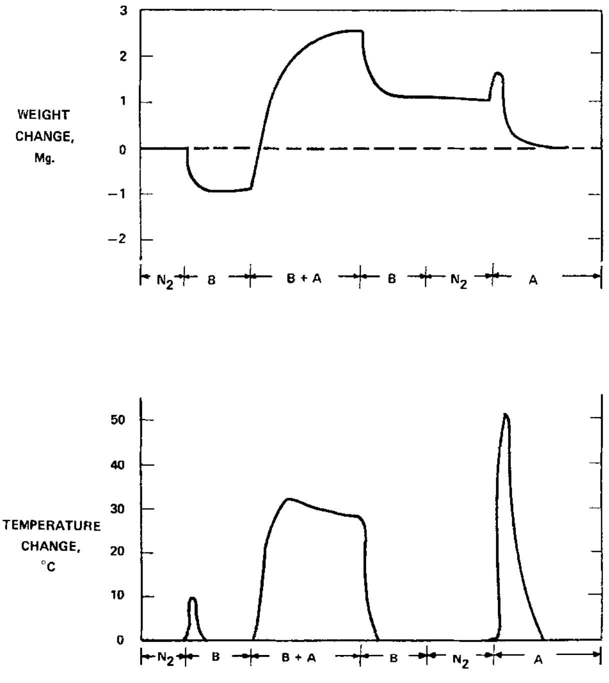

FIG. 4. Butene-air reaction with $ZnCrFeO_4$, 450 mg charge, 350°C, $B/O_2 = 1.5$. Symbols: A, air; B, butene.

by a large heat release. The later phenomena are typical of that found in coked catalyst regeneration studies (*12*).

The experiment just described permits deduction of the state of the catalyst during reaction in the presence of air. Figure 5 summarizes the various processes occurring in the first three steps of the experiment, i.e., the cycle involving butene, butene plus air, and butene. From previous analysis, we showed that reaction of the fresh catalyst (oxidized state) with butene resulted in catalyst oxygen loss and olefins adsorption, and the weight of oxygen lost was about three times that of olefin adsorbed. Thus, from the net weight obtained in the first step, we estimate that the catalyst lost 1.5 mg of oxygen. The same weight change was noted in going from the second to the third step when the air was removed. Since the catalyst is in the reduced state in the third step, it must have been predominantly in the oxidized state when air was present (second step) to account for the weight loss; the loss is much too large to be due to reversibly adsorbed hydrocarbon species, especially as no desorption occurred when the butene was removed. We conclude, therefore, that the operational state of the catalyst in the given butene-air mixture is essentially the oxidized form.

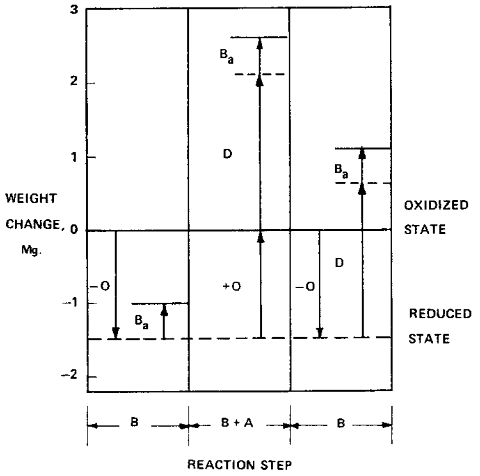

FIG. 5. Analysis of catalyst weight changes in butene-air experiment. Symbols: *A*, air; *B*, butene; B_a, adsorbed olefins; *D*, carbonaceous deposit; O, catalyst oxygen.

Fresh vs. Aged Catalyst

A zinc–chromium ferrite catalyst, which had been exposed to a butene-air mixture for a period of time, in fixed-bed reactor, was examined for structural or chemical differences compared to the fresh catalyst. The surface areas were essentially the same for both catalysts. The approach taken was to compare the reactivity of the fresh and aged catalyst (regenerated) towards butene in the microbalance. The results are shown in Table 2. The initial loss in weight after reaction with butene was the same for both catalysts. Interestingly, the initial rate of reaction in butene was considerably different; the aged catalyst reacted many times faster than the fresh one. The catalysts were regenerated in air again reacted with butene. For the second reduction, the weight losses were not markedly different. However, the fresh catalyst showed a faster subsequent reaction rate than initially; the magnitude was of the same order as that of the aged catalyst. It is known from X-ray diffraction data that the fresh catalyst contains a minor amount of uncombined oxides present in addition to the spinel structure. Magnetic susceptibility and Mossbauer studies have indicated that Fe^{3+} and Cr^{3+} cations present in the free-oxide phase are able to diffuse into the spinel lattice more readily in a hydrocarbon atmosphere than in air (*5*). Upon reoxidation, only the spinel phase remains. For the fresh catalyst, once the pure spinel structure is established, the surface reactivity towards butene approaches the level

TABLE 2
BUTENE REACTIVITY FOR FRESH VS. AGED $ZnCrFeO_4$ CATALYST

	450 mg charge, 350°C, 0.17 atm butene	
	Fresh	Aged
Surface area, m^2/g	1.6	1.9
First wt. loss, mg	0.46	0.42
Rate, mg/min	0.03	0.21
Second wt loss, mg	0.38	0.48
Rate, mg/min	0.21	0.31

of the aged catalyst which had a history of long-term butene exposure. Therefore, with the technique employed, there appears to be no significant difference in the surface reactivity of the fresh conditioned catalyst and the aged catalyst. Similar results were reported by Buyanov *et al.*, who found no marked differences between the phase compositions of fresh and aged Zn–Cr–Fe oxide catalysts (*3*).

DISCUSSION

There seems little doubt that oxidative dehydrogenation over metal oxides involves a redox cycle, with the metal cation reducing to a lower valence state due to reaction with the olefin, followed by reoxidation to the higher state with oxygen. An additive component which improves selectivity is thought to enhance the redox cycle by producing a new lattice structure or by more favorable alteration of the unit cell dimensions (*1*). In the case of zinc–chromium ferrite, undoubtedly the redox cycle involves Fe^{2+} and Fe^{3+}, as was confirmed by ESR measurements on the reduced catalyst. Iron oxide itself exhibits activity but rapidly declines owing to overreduction beyond the +2 state. The presence of chromium and zinc stabilizes the iron to deep reduction in the spinel enviroment. The results of hydrogen treatment and reactivity in butene are in accord with this picture. Catalytic stability of the oxide depends on being able to achieve reduction to the lower state without altering the lattice configurations so that upon reoxidation, the original state is obtained. If reduction is too severe, the compound oxide structure is destroyed, resulting in a mixture of simple oxides with concomitant demise in surface area (*6*). This probably is the case for the binary oxides of iron.

The action of butene on the oxides is considerably milder from a reducing point of view. Thus, intermediate states of reduction are generally obtained in this medium. For example, in iron oxide and chromium ferrite, bulk reduction of the iron to lower valence is obtained, whereas in zinc ferrite and zinc–chromium ferrite, reduction is confined to the surface layers. Nevertheless, the potential exists for deep reduction in the former catalysts; given sufficient time and proper conditions. It seems noteworthy that the two oxides which showed only surface reductions $ZnFe_2O_4$ and $ZnCrFeO_4$, exhibited the best selectivity for butadiene formation (*5*). Apparently, bulk reduction is detrimental to good selectivity, although other factors may operate here, such as propensity towards carbon formation, ease of reoxidation, lattice spacing, etc. Certainly, a stable bulk phase is a desirable property, providing an active surface is present.

In the case of zinc–chromium ferrite catalyst, only the surface layers are susceptible to reduction in butene. Our results showed the equivalent of two oxide layers removed, which we attribute to one lattice oxide layer and a chemisorbed oxygen layer. Many oxides strongly chemisorb oxygen, the excess oxygen being adsorbed on the surface or introduced into the oxide lattice directly in the layer next to the surface (*13*). The latter process creates vacancies which may be active sites for olefin adsorption. It is probable that a portion of the excess chemisorbed oxygen is in the form of O^- (*14*, *15*), charge compensation being realized by concomitant surface oxidation of Cr^{3+} to Cr^{6+} (*16*). A sorbed, charged oxygen species has been suggested to be the active intermediate in the selective oxidation of propylene to acrolein on cuprous oxide (*17*). The radical-ion concentration probably only constitues a small fraction of the surface layer (*18*).

In line with these thoughts, we advance the proposed scheme of surface reactions shown in Fig. 6 for the oxidative dehydrogenation of butene in the presence of oxygen. The essential reactions have already been discussed (*5*). The active center for butene adsorption is postulated to be a group, where □ is an anion vacancy, and O^- is a sorbed oxygen radical ion. Hydrogen abstraction from the adsorbed butene creates a C_4H_7 fragment and an OH^- group. Reversibility of this step may account for

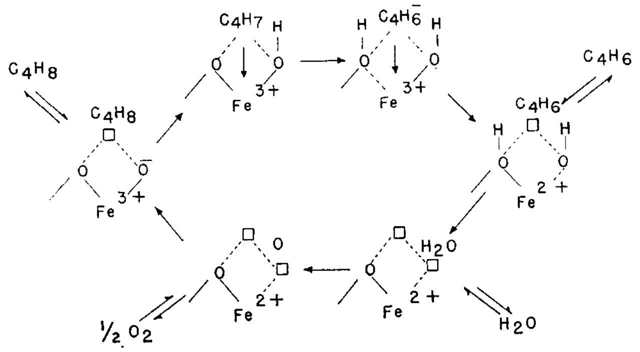

FIG. 6. Proposed surface reactions for butene oxidation.

butene isomerization. A second hydrogen abstraction forms butadiene, which is subsequently desorbed, and another OH^- group. During this step, the iron becomes reduced to the $+2$ valence state. Two OH^- groups combine to generate water and reform a lattice oxide. The reduced iron is now reoxidized by oxygen from the gas phase (or neutrally-charged adsorbed oxygen) reforming the original catalyst center. Although the active center is considered a specific group of atoms, it should be noted that according to the reaction sequence envisaged there are two adsorption sites in the center; viz., one for butene and one for oxygen. Butene, as an allylic intermediate, is considered coordinated to the iron via π-bonding while oxygen, as an adsorbed ion radical, occupies a surface anion vacancy in the spinel oxide layer.

The proposed sequence formally parallels that of Schuit *et al.* (*18*) for the oxidation of butene over bismuth-molybdate catalyst. However, an important difference resides in in the first hydrogen-abstraction step; we envisage a homolytic dissociation with the hydrogen attaching to the O^- radical instead of the lattice O^{-2} in Schuit's scheme. This is necessary to avoid a two-step reduction in the iron valence as occurs with molybdenum in Schuit's mechanism. The second hydrogen abstraction is heterolytic, forming the Fe^{3+}–$C_4H_6^-$ complex, which dissociates with reduction of the iron to Fe^{2+} and desorption of butadiene.

Kinetic analysis of fixed-bed runs on the oxidative dehydrogenation of butene-1 to butadiene over zinc–chromium ferrite catalyst indicated the rate of reaction under normal operating conditions to be approximately zero order in both butene and oxygen, and negative first order in butadiene (*19*). This suggests that the catalyst surface is fully covered with olefin and with oxygen, each on different sites. This is in agreement with out results and in accord with our picture of the active center. Product inhibition may be accounted for by competition for adsorption between butene and butadiene, their sum remaining constant at essentially full coverage.

It remains to discuss catalyst stability for the butene reaction with oxygen present in the feed. It is true, of course, in this case, that provided the proper olefin to oxygen ratio is maintained, catalyst reduction—oxidation should be confined to the surface layer. Nevertheless, severe aging and loss of selectivity were obtained for those oxides which showed bulk reducibility in butene alone (*5*). This may have been due to excessive coking, but more likely signifies bulk catalyst reduction is occurring even in the presence of oxygen (*4*). Selectivity changes in aged (reduced) catalysts have been ascribed to the slowness of the reoxidation step, necessitating that the olefin react with intermediate oxygen ions or molecular oxygen itself (*1*). It appears that the zinc–chromium ferrite catalyst avoids these vagaries by virture of the stability of the bulk structure to reduction, while maintaining a reactive surface.

CONCLUSIONS

The present investigation supports the following conclusions:

(1) The ease of reducibility of the oxides of Zn, Cr, and Fe in hydrogen decreases in the order:

$$Fe_2O_3 > ZnFe_2O_4 > ZnCrFeO_4 = FeCrO_3 > ZnCr_2O_4 > ZnO > Cr_2O_3.$$

(2) In butene, Fe_2O_3 and $FeCrO_3$ undergo bulk reduction to lower-valence oxides, while $ZnFe_2O_4$ and $ZnCrFeO_4$ undergo surface reduction only.

(3) Reduction of $ZnCrFeO_4$ in butene removes approximately two monolayers of oxygen; one is ascribed to chemisorbed oxygen and the other to lattice oxide.

(4) In butene and air, the $ZnCrFeO_4$ catalyst remains in the oxidized state; a carbonaceous deposit rapidly forms but then lines out during the exothermic catalytic reaction.

A surface reaction sequence for the oxidation of butene to butadiene over $ZnCrFeO_4$ catalyst, which involves an iron–oxygen radical active center, is proposed.

ACKNOWLEDGMENTS

The authors are indebted to Mr. W. E. Faust for the microbalance experiments, to Dr. K. S. Seshadri for the ESR measurements, and to Mr. W. L. Kehl for X-ray analyses and helpful discussions on structural aspects of the catalysts.

REFERENCES

1. CULLIS, C. F., *Ind. Eng. Chem.* **59,** 18 (1967).
2. BATIST, PH. A., LIPPENS, B. C., SCHUIT, G. C. A., *J. Catal.* **5,** 55 (1966).
3. BUYANOV, R. A., ANDRUSHKEVICH, M. M., KARAKCHIEV, L. G., *Kin. Catal. (USSR)* **6,** 966 (1965).
4. SKARCHENKO, V. K., *Int. Chem. Eng. Process, Ind.* **9,** 1 (1966).
5. RENNARD, R. J., JR., KEHL, W. L., preceding paper.
6. POSPISIL, M., CABICAR, J., *Collect. Czech. Chem. Commun.* **32,** 3832 (1967).
7. GARNER, R. A., *Proc. Int. Congr. Catal. 4th* Moscow, Preprint No. 83 (1968).
8. MASSOTH, F. E., unpublished data.
9. MASSOTH, F. E., AND MENON, P. G., *Ind. Eng. Chem. Process Des. Develop.* **8,** 383 (1969).
10. POOLE, C. P., JR., DICARLO, E. N., NOBLE, C. S., ITZEL, J. F., JR., TOBIN, H. H., *J. Catal.* **4,** 518 (1965).
11. MCCLELLAN, A. L., AND HARNSBERGER, H. F., *J. Colloid Interface Sci.* **23,** 577 (1967).
12. MASSOTH, F. E., *Ind. Eng. Chem. Process Des. Develop.* **6,** 200 (1967).
13. BIELANSKI, A., DEREN, J., AND VOLTER, M., *Kin. Catal. (USSR)* **5,** 743 (1964).
14. RIDEAL, E. K., "Concepts in Catalysis," p. 86. Academic Press, N. Y., 1968.
15. BLIZNAKOV, G., MEHANDJIEV, D., ELAZAROVA, F., *Dokl. Bolg. Akad. Nauk.* **19,** 385 (1966).
16. SHENDRIK, M. N., AND USACHEVA, N. S., *Khim. Prom. (Moscow)* **45,** (3), 194 (1969); *Chem. Abstr.* **71,** 6879f (1969).
17. WOOD, B. J., WISE, H., AND YOLLES, R. S., *J. Catal.* **15,** 355 (1969).
18. SCHUIT, G. C. A., *Chim. Ind. (Milan)* **51,** 1307 (1969).
19. STERRETT, J. S., unpublished data.